ELSEVIER

Soil Dynamics and Earthquake Engineering 23 (2003) 383–389

SOIL DYNAMICS AND EARTHQUAKE ENGINEERING

www.elsevier.com/locate/soildyn

Seismic soil–structure interaction of massive flexible strip-foundations embedded in layered soils by hybrid BEM–FEM

C.C. Spyrakos[a,*], Chaojin Xu[b]

[a]*Laboratory of Earthquake Engineering, Department of Civil Engineering, National Technical University of Athens, Polytechnic Campus Zografos, Athens 15700, Greece*
[b]*Algor Inc., 150 Beta Drive, Pittsburgh, PA 15238, USA*

Accepted 27 December 2002

Abstract

A study on the seismic response of massive flexible strip-foundations embedded in layered soils and subjected to seismic excitation is presented. Emphasis is placed on the investigation of the system response with the aid of a boundary element–finite element formulation proper for the treatment of such soil–structure interaction problems. In the formulation, the boundary element method (BEM) is employed to overcome the difficulties that arise from modeling the infinite soil domain, and the finite element method (FEM) is applied to model the embedded massive flexible strip-foundation. The numerical solution for the soil–foundation system is obtained by coupling the FEM with the BEM through compatibility and equilibrium conditions at the soil–foundation and soil layer interfaces. A parametric study is conducted to investigate the effects of foundation stiffness and embedment on the seismic response.

Keywords: Flexible strip-foundations; Soil–structure interaction; Seismic response; Boundary element method; Finite element method

1. Introduction

During the last decades, several methods have been developed to consider the effects of soil–structure interaction (SSI) on the response of structures subjected to seismic waves [1,2].

Extensive research has been conducted on analytical or semi-analytical methods. However, the application of such methods is very limited since solutions are only available for systems with simple geometry. With the help of modern computer technology, numerical methods have been developed to treat complexities involving SSI, [3]. In applying the finite element method (FEM) to SSI analysis, however, special boundaries, such as transmitting boundaries, have been devised to overcome the difficulties in modeling the semi-infinite soil domain, [4]. A hybrid formulation has been developed by Romanel and Kundu [5] to study the response of deeply embedded structures in a multilayered half space for P and SV waves.

An alternative approach is the hybrid finite element–boundary element method (FEM–BEM). In this method, the FEM is utilized to model the foundation and the 'near-field' of the soil, and the BEM is employed to model the 'far-field' of the soil domain since it automatically satisfies the 'far-field' boundary conditions associated with the semi-infinite soil domain [6]. Another advantage of this method over the FEM is that it reduces the dimensions of the problem by one, and thus saves modeling and processing time.

A generally adopted methodology that considers SSI in seismic analysis consists of three steps. First, the seismic waves in the free field prior to any excavation of the soil portion are determined based on wave propagation theory. Then, the so-called scatter field motion with the soil portion excavated that lies on the interface between 'near-field' and 'far-field' interface, usually the soil–structure contact interface, is computed from the free-field seismic waves. Finally the seismic response of the structure is obtained using the scatter motion [6]. Because of the complexity of the problem, most of the studies regarding the SSI of soil–foundation systems subjected to seismic excitation have been limited to foundations on homogeneous viscoelastic half-space. Representative are the works of Wolf [7] and Avilez and Perez-Rocha [8] who have studied the case of rigid rectangular foundations

* Corresponding author. Tel./fax: +30-1-699-0044.
E-mail address: spyrakos@hol.gr (C.C. Spyrakos).

0267-7261/03/$ - see front matter © 2003 Elsevier Science Ltd. All rights reserved.
doi:10.1016/S0267-7261(03)00019-8

while Whittaker and Christiano [9] considered flexible rectangular foundations. Formulations for rigid strip-foundations have been presented by Abascal and Dominguez [10], Spyrakos and Beskos [11], and the response of surface flexible strip-foundations on a homogeneous half-space has been investigated by Spyrakos and Beskos [12], and Kokkinos and Spyrakos [13].

To perform a SSI analysis of flexible strip-foundations embedded in layered soils subjected to seismic excitations, a hybrid BEM–FEM formulation is presented. The seismic excitations are prescribed at the bedrock-soil interface. In the hybrid BEM–FEM formulation, the flexible foundation is modeled with finite elements, while the infinitely extended soil is modeled with boundary elements. The governing equation is derived by enforcing compatibility and equilibrium conditions at the soil–foundation and soil layers interface. A series of convergence studies are conducted to obtain the optimum meshes of the boundary discretization. The seismic response of foundations subjected to P-waves and S-waves is investigated. Numerical examples are presented to assess the effects of foundation stiffness and embedment on the seismic response of the soil–foundation system.

2. Formulation and numerical treatment

The system consists of a flexible strip-foundation embedded in layered soil (see Fig. 1). The soil–structure interface is indicated by 'c', and the top soil layer boundaries as 'e', 'c', and 'l'. The boundary 'e' is the free surface and the boundary '1' is the contact interface with the soil layer [2]. The bottom layer has a top boundary $n-1$ which is the contact interface with layer $[n-1]$ and a bottom boundary n which is the interface with the bedrock. In general, a layer $[k]$ has a top boundary $k-1$ and a bottom boundary k, where $k-1$ and a bottom boundary k, where $k-l$ is the interface between layers $[k-l]$ and $[k]$.

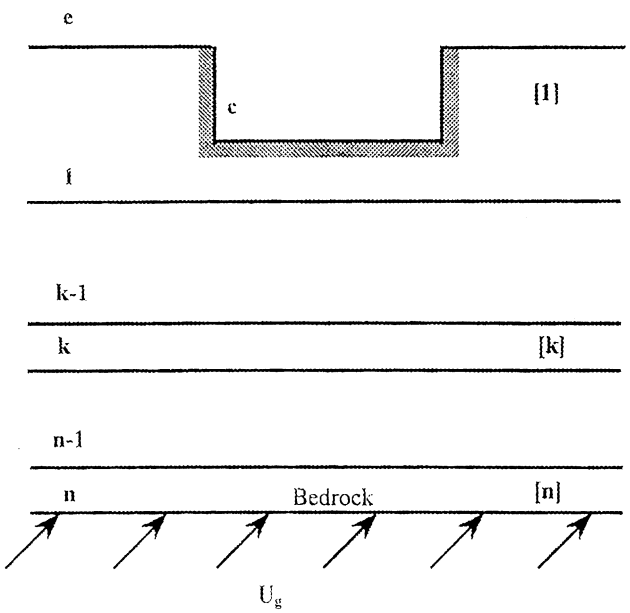

Fig. 1. Foundation embedded in layered soil.

2.1. BEM formulation for the soil

Assuming small displacements and soil layers that are homogeneous, isotropic, and linearly elastic, the governing equations for each layer are the Navier's equations. Expressed in terms of displacements in the frequency domain, Navier's equation is given by

$$(c_1^2 - c_2^2)U_{i,ij} + c_2^2 U_{j,ii} - k^2 U_j = 0 \tag{1}$$

where $k = \mathrm{i}\omega$, ω is the circular frequency of the seismic excitation, and

$$c_1 = \sqrt{\frac{E_s(1-\nu_s)(1-2\xi_i)}{\rho_s(1+\nu_s)(1-2\nu_s)}}$$
$$c_2 = \sqrt{\frac{E_s(1+2\xi_i)}{2\rho_s(1+\nu_s)}} \tag{2}$$

are P- and S-wave velocities, respectively. In Eq. (2), E_s, ρ_s and ν_s are the modulus of elasticity, the mass density and the Poisson's ratio, respectively, and ξ is introduced to include the effect of hysteretic damping [6].

The corresponding boundary conditions to Eq. (1) are

$$U_i(\vec{x};k) = F_i(\vec{x};k) \qquad \vec{x} \in \Gamma_1$$
$$T_i(\vec{x};k) = G_i(\vec{x};k) \qquad \vec{x} \in \Gamma_2 \tag{3}$$

where $F_i(\vec{x},k)$ and $G_i(\vec{x},k)$ are known displacements and tractions on the boundaries Γ_1 and Γ_2.

Eq. (1) together with the boundary conditions (3) is numerically solved using BEM.

The numerical solution requires discretization of the soil layers and soil–foundation interfaces. As extensively elaborated in Ref. [14], the boundary of a typical layer is divided into N boundary elements ($l = 1, 2, \ldots, N$). Using constant boundary elements and applying Dirac's delta function successively to the element nodes, one obtains a set of $2 \times N$ linear equations that relate the displacements to tractions, that is

$$[H]\{U^s\} = [G]\{T^s\} \tag{4}$$

where $[H]$ and $[G]$ are $2N \times 2N$ matrices that correspond to the fundamental solutions as elaborated in Refs. [14,15], $\{U^s\}$ and $\{T^s\}$ are the nodal displacement and traction vectors, respectively. A detailed description of the methodology can be found in Xu [14] and Dominguez [15].

In order to obtain the equilibrium equation of the soil–foundation system, the tractions $\{T^s\}$ in Eq. (4) must be expressed in terms of the nodal forces $\{F^s\}$. The matrix

manipulations to derive Eq. (5) are presented in detail in Ref. [14].

$$[K^s]\{U^s\} = \{F^s\} \tag{5}$$

where

$$[K^s] = [L][G]^{-1}[H] \tag{6}$$

$$\{F^s\} = [L]\{T^s\} \tag{7}$$

in which

$$[L] = \text{diag}\{l_1 l_1 l_2 l_2 \bullet\bullet\bullet l_N l_N\} \tag{8}$$

where l_i is the length of the ith boundary element.

2.2. FEM formulation for the strip-foundation

The thickness h of the foundation is small compared to the other dimensions of the foundation. which justifies the use of thin plate elements to model the foundation. The Mindlin-Kirkorff plate theory is utilized in the FEM formulation for the strip-foundation [16]. According to this theory, the governing equations for bending and axial deformation are uncoupled.

Following standard FEM procedures, the strip-foundation is divided into M elements and the equilibrium equation relating nodal forces to displacements can be written in the form [17,18]

$$\begin{bmatrix} D_{uu} & D_{u\theta} \\ D_{\theta u} & D_{\theta\theta} \end{bmatrix} \begin{Bmatrix} U^f \\ \theta \end{Bmatrix} = \begin{Bmatrix} F^f \\ M \end{Bmatrix} \tag{9}$$

where the subscripts u and θ refer to the nodal displacements and rotations, respectively. The stiffness coefficients in Eq. (9) can be found in Ref. [17]. Through condensation of the rotational degrees-of-freedom, Eq. (9) can be rewritten in the following form [14]

$$\{F^f\} = [K^f]\{U^f\} \tag{10}$$

where

$$[K^f] = [D_{uu}] - [D_{u\theta}][D_{\theta\theta}]^{-1}[D_{\theta u}] \tag{11}$$

3. Coupling of BEM with FEM

The system equation can be obtained by enforcing compatibility and equilibrium conditions at the soil–foundation and soil layer interfaces. Specifically, at the interfaces, the displacements of each sub-structure are the same, that is

$$\begin{aligned} &\{U_e^s\} = \{U_e\} \\ &\{U_c^s\} = \{U_c^f\} = \{U_c\} \\ &\{U_i^s\} = \{U_{i-l}^s\} = \{U_i\} \\ &\{U_n^s\} = \{U_g\} \end{aligned} \tag{12}$$

in the absence of external forces, the forces acting on each substructure sum up to zero, that is

$$\begin{aligned} &\{F_e^s\} = \{0\} \\ &\{F_c^s\} + \{F_c^f\} = \{0\} \\ &\{F_{il}^s\} + \{F_i^s\} = \{0\} \end{aligned} \tag{13}$$

where the displacement vectors without superscript indicate the common displacement at the interfaces, while 'f' and 's' indicate structure and soil interfaces, respectively, and U_g represents the seismic excitation prescribed at the bedrock interface. Subscripts denote the interfaces of the soil layers as shown in Fig. 1.

Combining the equilibrium equations for each substructure, and employing the compatibility conditions at the interfaces, the equilibrium equation for the system is obtained [14,15] where

$$[K]\{U\} = \{F\} \tag{14}$$

4. Numerical examples

In the following discussion and numerical examples, the seismic excitations are prescribed at the bedrock interface. Two different harmonic excitations are considered: the first one is a P-wave with only a unit vertical component normal to the bedrock interface, and the second one is a S-wave with only a unit horizontal component along the bedrock interface. As shown in Fig. 2, the system consists of a foundation with a width $2B = 4$ m embedded in a soil layer with a depth H over a half-space bedrock. The depth of the embedment is D and the ratio of foundation width to thickness of the soil layer if $H/B = 2$. The material properties of the soil are: modulus of elasticity $E_s = 100 \times$ MPa, mass density $\rho_s = 2000$ kg/m^3, Poisson's ratio $\nu_s = 0.33$, and damping ratio $\xi_s = 0.05$. The material properties of the foundation are: mass density $\rho_f = 2500$ kg/m^3, Poisson's ratio $\nu_f = 0.3$, and damping ratio $\xi_f = 0.05$.

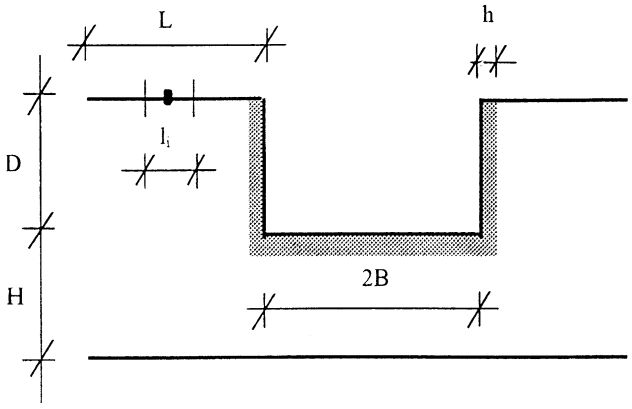

(a)

Fig. 2. Dimensions of soil–foundation system.

4.1. Effect of foundation stiffness

According to the paper by Kokkinos and Spyrakos [13], the relative stiffness K_r and mass density M_r for a foundation–soil system are defined as

$$K_r = \frac{E_f h^3}{1-\nu_f^2} \times \frac{1+\nu_s}{E_s B^3} \tag{15}$$

$$M_r = \frac{\rho_f}{\rho_s} \tag{16}$$

Foundations with relative stiffness of 500, 5, 0.05 correspond to rigid, intermediate, and very flexible foundations, respectively [13]. To evaluate the effect of foundation stiffness on the response, two foundation–soil systems with relative stiffness 45 and 0.045 are considered. The corresponding moduli of elasticity for the foundations are $E_f = 10^6$ MPa and $E_f = 10^3$ MPa yielding $K_r = 45$, a stiff foundation, and $K_r = 0.045$, a soft foundation, respectively.

In all the numerical examples, the results are presented in relative displacement, U_r, that is

$$U_r = \frac{U}{U_g} \tag{17}$$

where U is the displacement response at free surface, with respect to the nondimensionless frequency A_0, that is defined by

$$A_0 = \frac{B\omega}{c_2} \tag{18}$$

where ω is the circular frequency of the harmonic excitation.

For the stiff foundation, the relative vertical displacements along the top surface from the foundation center for harmonic P-waves are shown in Fig. 3. Fig. 4 depicts the relative horizontal displacements along the top surface from the foundation center for S-waves. Results for the vertical displacements can be found in Ref. [14]. As elaborated in Ref. [14], the relative displacements for the soft foundation remain practically constant along the top free surface. Specifically, for a P-wave, the horizontal displacement is negligible and the vertical displacement remains uniform at the top free surface, while for a S-wave, the vertical displacement is negligible and the horizontal displacement remains constant. The relative vertical displacements at the foundation center for both soft and stiff foundations subjected to P-waves are plotted in Fig. 5 and those for S-waves are drawn in Fig. 6

Figs. 5 and 6 clearly indicate that the main difference of the top free surface displacement for the seismic excitation at the bedrock interface is that the amplitude is amplified for the soft foundations. However, as demonstrated in Figs. 3 and 4, the stiff foundation greatly modifies the propagation pattern of the wave away from the center of the foundation. Though at a low excitation frequency range, e.g. $A_0 = 0.5$, a frequency lower than the fundamental frequency (see Figs. 5

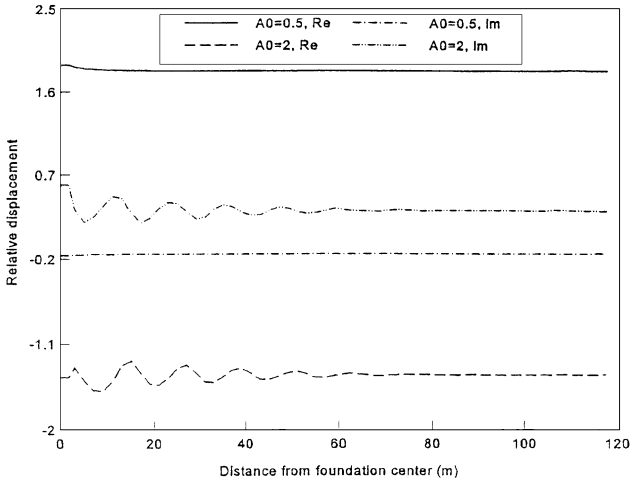

Fig. 4. Horizontal displacement at top surface for stiff foundation to S-waves.

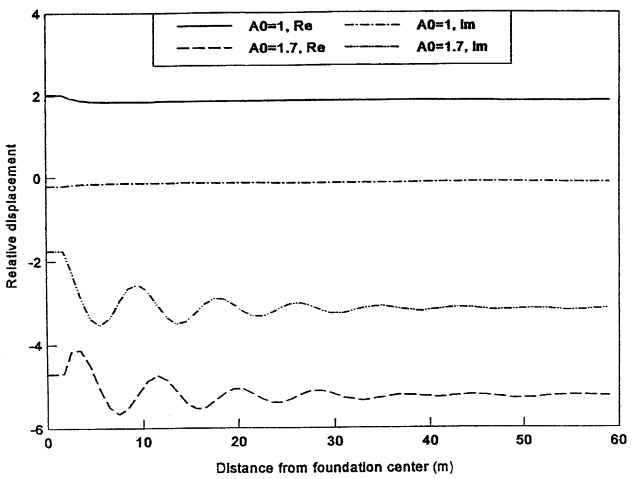

Fig. 3. Vertical displacement at top surface for stiff foundation to P-waves.

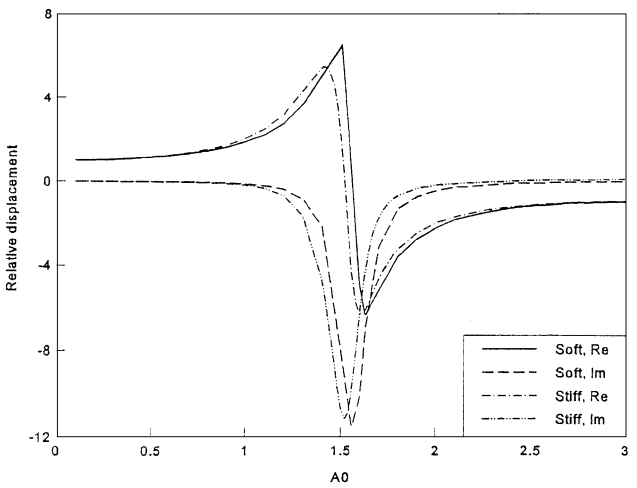

Fig. 5. Effects of foundation stiffness for surface foundation to P-waves.

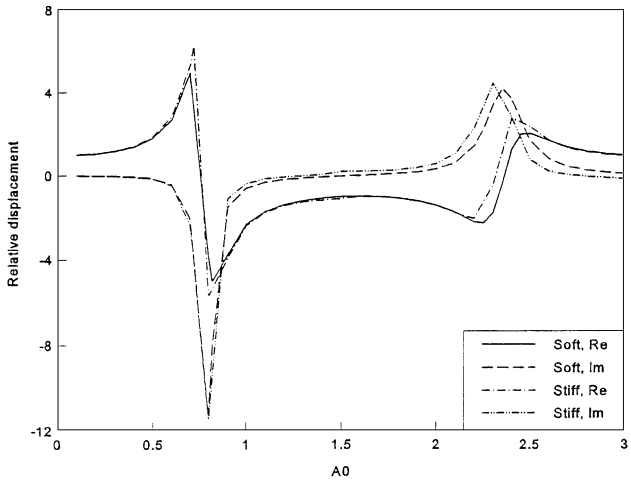

Fig. 6. Effects of foundation stiffness for surface foundation to S-waves.

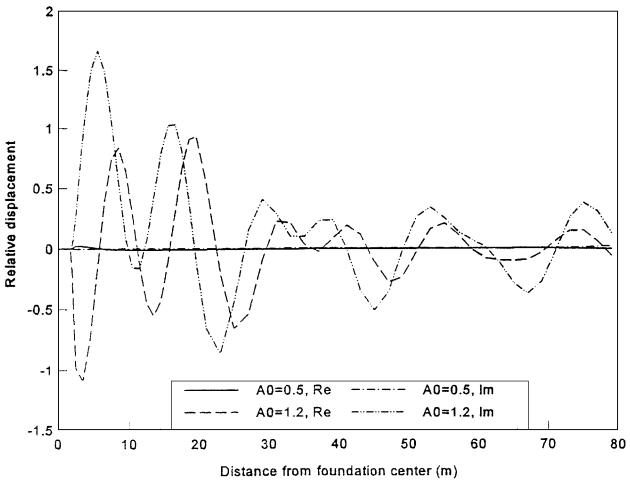

Fig. 7. Horizontal displacement at top surface to P-waves ($D = 2$ m).

and 6), the modification is not significant, at frequencies higher than the fundamental, e.g. $A_0 = 2$, the wave pattern is altered. As can be observed in Figs. 3 and 4, the vertical displacement amplitude for the foundation subjected to a P-wave and the horizontal displacement amplitude for the foundation subjected to a S-wave are no longer constant at the top free surface and a standing wave caused by SSI develops at the top free surface. Also, the horizontal displacement for the P-wave excitation and the vertical displacement component for the S-wave are no longer negligible compared to the corresponding vertical and horizontal components, respectively [14].

A detailed discussion and parametric studies on the behavior of surface foundations placed on a two-layer soil over bedrock are presented in Ref. [14].

4.2. Effect of foundation embedment

In the examples, the system parameters are given the values assigned in Section 4.1. All foundations are characterized by a modulus of elasticity $E_f = 10^6$ MPa, that is the foundation stiffness is kept constant. A detailed discussion on the variation of both foundation stiffness an embedment is presented in Ref. [14].

4.2.1. Foundations subjected to P-waves

Two foundations with embedments $D = 2$ m and $D = 4$ m are considered together with the surface foundation described in the previous section. The horizontal components of the relative displacement at the top surface from the foundation center are shown in Fig. 7 for $D = 2$ m, and in Fig. 8 for $D = 4$ m. The real and imaginary components of the vertical relative displacement components at the foundation center are plotted in Fig. 9. In Figs. 7 and 8, notice that at a low frequency, e.g. $A_0 = 0.5$, a frequency that is smaller than any of the fundamental frequencies for the three cases that are examined, which as depicted in Fig. 9 lie in the 0.7–1.5 range, the system responds as if there is no foundation. Specifically, the horizontal displacement is negligible compared to vertical displacement, and each point on the free surface shows a uniform vertical displacement for low frequencies. When the excitation frequency exceeds the natural frequency, the system responds differently due to the presence of the foundation. Parametric studies have shown that the number of standing waves is usually less than six [14].

As expected in Fig. 9, the deeper the foundation embedment, the lower the natural frequency of the system. More importantly, as one can see from Fig. 9, the embedment has a beneficial effect on displacement amplitudes. Though the real part of the vertical relative displacement component is almost the same for the three foundations, an increase of the embedment decreases the imaginary part of the response. The imaginary part of the foundation with $D = 2$ m is only 70% than that of the surface foundation, while the imaginary part of the foundation with $D = 4$ m is only 40% than that of

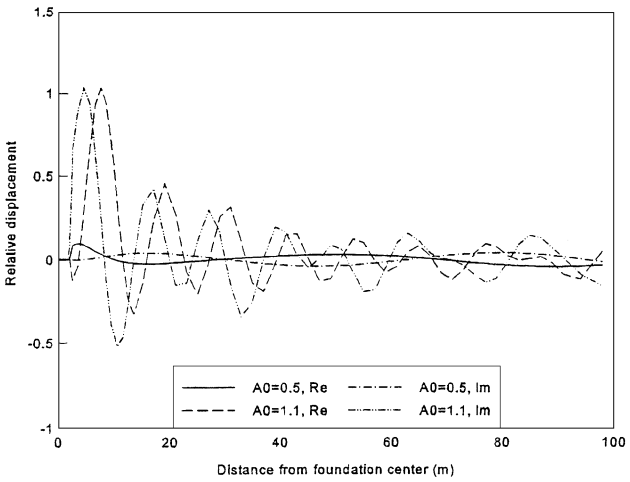

Fig. 8. Horizontal displacement at top surface to P-waves ($D = 4$ m).

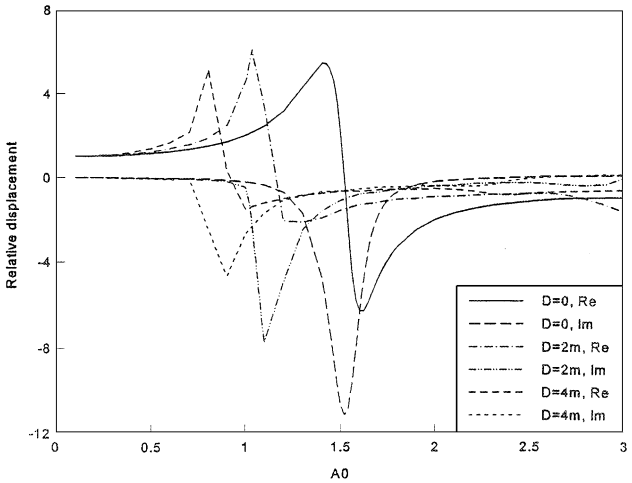

Fig. 9. Effects of foundation embedment to P-waves.

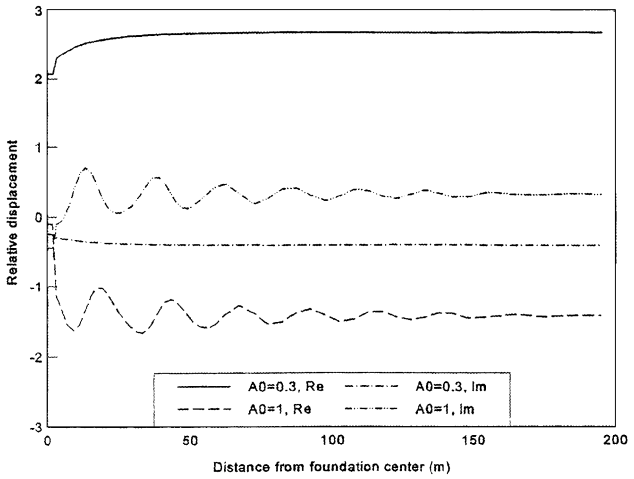

Fig. 11. Horizontal displacement at top surface to S-waves ($D = 4$ m).

the surface foundation, which clearly indicates the effect of foundation embedment on radiation damping.

4.2.2. Foundations subjected to S-waves

As in the previous example, three foundations with $D = 0$, $D = 2$ m, and $D = 4$ m are studied to assess the effect of foundation embedment on the seismic response for S-waves. The horizontal components of the relative displacement along the top surface from the foundation center are shown in Figs. 4, 10, and 11 for foundations with $D = 0.2$ m, and 4 m, respectively. The horizontal relative displacement components at the foundation center are plotted in Fig. 12 versus the nondimensionless frequency A_0.

The foundation response exhibits similar behavior to P-waves. The effect of the embedment is not significant for frequencies lower than the fundamental frequency. However, it becomes more important when the excitation frequency exceeds the fundamental frequency. The standing wave due to SSI travels about six standing waves and then disappears [14]. Also, increasing the foundation embedment enhances the SSI effect. Specifically, the presence of sidewalls reduces the displacements demonstrating that the deeper the embedment, the smaller the displacement. As shown in Fig. 12, both the real (Re) and the imaginary (Im) parts of the displacement are reduced to a similar degree because of an increase of foundation embedment. The displacement reduction of foundation with $D = 2$ m is 30% from that of the surface foundation, and the displacement reduction for foundation with $D = 4$ m is 4% from that of the surface foundation.

Comparing the response due to P-waves with S-waves, notice that the fundamental frequency of the system for S-waves is only half of the system's fundamental frequency for P-waves. Though the standing wave disappears after six circles for both P and S-waves, the standing wave for a S-wave travels twice the distance of that for a P-wave, which implies that a larger area at the free surface

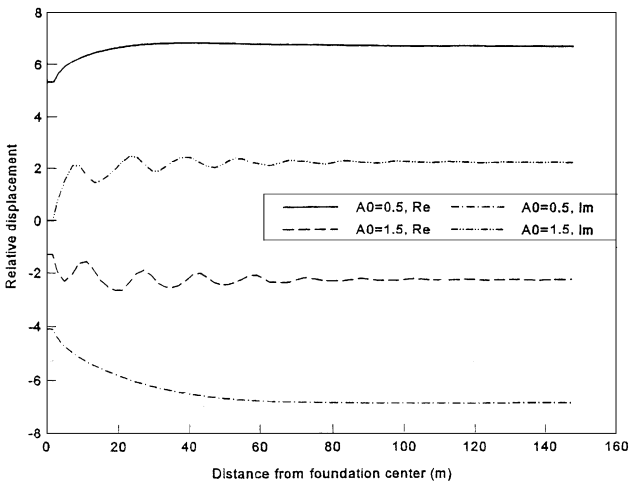

Fig. 10. Horizontal displacement at top surface to S-waves ($D = 2$ m).

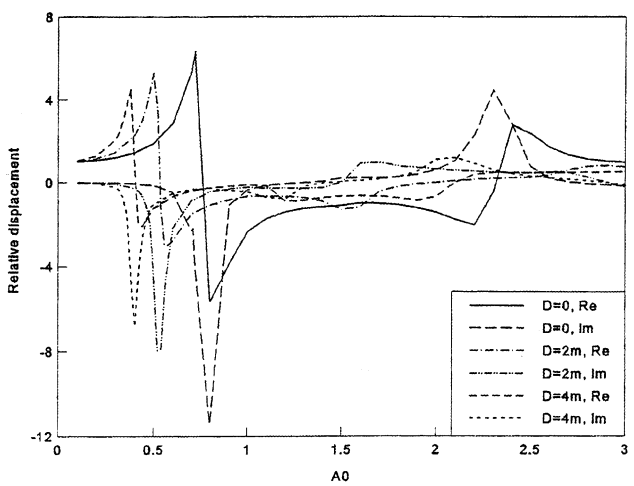

Fig. 12. Effects of foundation embedment to S-waves.

surrounding the foundation should be discretized to capture the effect of S-waves on foundation response [13].

5. Conclusions

A study has been presented for the SSI analysis of flexible strip-foundations embedded in layered soils subjected to plane P-waves and S-waves. To simplify the formulation, the seismic excitations are prescribed at the bedrock interface. The numerical formulation is based on coupling of the BEM and FEM methods.

Through parametric studies the effect of foundation flexibility and embedment are investigated. It is demonstrated that SSI plays an important role and should be considered for both surface and embedded foundations when the difference of the stiffness between the foundation and the soil is large. A few significant observations include: when the excitation frequency exceeds the fundamental frequency of the soil–foundation system, the response of soft foundations shows considerable difference from that of stiff foundations. The foundation embedment has a beneficial effect on the displacement response, since it can lead to dramatic reductions. Indications are reductions of the displacements in the order of 60–70% from those of surface foundations.

References

[1] Antes H, Spyrakos CC. Soil–structure interaction. In: Beskos DE, Anagnostopoulos SA, editors. Analysis and design of earthquake resistant structures: a handbook. Southampton, UK: Computational Mechanics Publications; 1997. p. 271–332. Chapter 6.

[2] Coda HB, Venturini WS, Aliabadi MH. A general 3D BEM/FEM coupling applied to elastodynamic continua/frame structures interaction analysis. Int J Numer Meth Engng 1999;46(5): 695–712.

[3] Lysmer J, Udaka T, Seed HB, Hwang R. LUSH—a computer program for complex response analysis of soil—structure systems, Report EERC 74-4. Berkeley: University of California; 1974.

[4] Murakami H, Shioya S, Yamada R, Luco JE. Transmitting boundary for time harmonic elastodynamic of infinite domains. Int J Numer Meth Engng 1981;17:1697–716.

[5] Romanel C, Kundu T. A hybrid modeling of soil–structure interaction problems for deeply embedded structures in a multilayered medium. Earthquake Engng Struct Dyn 1993;22:557–71.

[6] Wolf JP. Dynamic soil–structure interaction. Englewood Cliffs, NJ: Prentice-Hall; 1984.

[7] Wolf J. Spring-dashpot-mass models for foundation vibration. Earthquake Engng Struct Dyn 1997;26:931–49.

[8] Avilez J, Perez-Rocha J. Effects of foundation embedment during building–soil interaction. Earthquake Engng Struct Dyn 1998;27: 1523–40.

[9] Whittaker WL, Christiano P. Response of a plate and elastic half-space to harmonic waves. Earthquake Engng Struct Dyn 1982;10: 255–66.

[10] Abascal R, Dominguez J. Dynamic response of embedded strip-foundation subjected to obliquely incident waves. Proc 7th Int Conf Boundary Elements, Lake Como, Italy, Section 6 1985;63–9.

[11] Spyrakos CC, Beskos DE. Dynamic response of rigid strip-foundations by time domain element method. Int J Numer Meth Engng 1986;23:1547–65.

[12] Spyrakos CC, Beskos DE. Dynamic response of flexible strip-foundations by boundary and finite elements. Soil Dyn Earthquake Engng 1986;5(2):84–96.

[13] Kokkinos FT, Spyrakos CC. Dynamic analysis of flexible strip-foundations in the frequency domain. Comput Struct 1991;39(5): 473–82.

[14] Xu CJ. Dynamic soil–structure–fluid interaction by hybrid FEM-BEM. PhD Dissertation, West Virginia University, WV, Morgantown; 1995.

[15] Dominguez J. Boundary elements in dynamics. New York: CMP & Elsevier Applied Science; 1993.

[16] Ugural AC. Stresses in plates and shells. New York: McGraw-Hill; 1981.

[17] Spyrakos CC, Beskos DE. Dynamic response of frameworks by fourier transform. J Comput Struct 1982;15:495–505.

[18] Spyrakos CC. Finite element modeling in engineering practice. Pittsburgh, PA: Algor Publishing Division; 1994.